Nano Research 2018, 11(7): 3648–3657
https://doi.org/10.1007/s12274-017-1931-6
Research Article

ISSN 1998-0124
CN 11-5974/O4

Flavonoid moiety-incorporated carbon dots for ultrasensitive and highly selective fluorescence detection and removal of Pb^{2+}

Jing Xu, Xu Jie, Fengfeng Xie, Haimei Yang, Weili Wei (✉), and Zhining Xia

School of Pharmaceutical Sciences and Innovative Drug Research Centre, Chongqing University, Chongqing 400013, China

Received: 12 April 2017
Revised: 16 November 2017
Accepted: 21 November 2017

KEYWORDS
flavonoid,
carbon dot,
fluorescence,
lead ion,
removal

ABSTRACT

A new type of self-targeting carbon dot (CD-Fla) for the detection of the toxic heavy metal ion Pb^{2+} was synthesized via a one-pot hydrothermal route using flavonoid extracts of *Ginkgo biloba* leaves as the starting material. As-prepared CD-Fla exhibited excellent biocompatibility and strong blue emission with a quantum yield of 16.1% and significant fluorescence quenching selectivity for Pb^{2+} without using any additional targeting molecules. CD-Fla could detect Pb^{2+} quantitatively within the range 0.1–20.0 nM, with an ultrahigh sensitivity of 55 pM. The selectivity of CD-Fla for Pb^{2+} was nearly one order of magnitude higher than that for other relevant metal ions. This was much better than ever reported CD-based metal ion sensors. The high sensitivity and selectivity were due to the incorporation of certain flavonoid-like moieties into CD-Fla. CD-Fla was also demonstrated to be a good probe for fluorescence tracing of intracellular Pb^{2+}. The capability of CD-Fla was further improved when it was doped on agarose hydrogel. CD-Fla-doped agarose hydrogel (CD-AHG) allowed for visual fluorescence detection and removal of Pb^{2+} from water. This was confirmed by testing CD-AHG in actual water samples taken from the Jialing River (Chongqing, China). The Pb^{2+} adsorbed CD-AHG was regenerable in HCl solution. This study will open a new avenue for synthesizing intelligent materials capable of simultaneously targeting, detecting, and treating heavy metal ions.

1 Introduction

Lead is a highly toxic heavy metal that accumulates in both water bodies and soil organisms [1, 2]. Exposure to even low concentrations of lead may lead to serious health problems such as damage to the central nervous system, reduced fertility in men, and diminished learning ability in children [3, 4]. Lead is released into the environment as a result of both natural processes and human activities, including fuel combustion, industrial processes, and solid waste combustion. One of the major concerns in this regard is the

Address correspondence to wlwei@cqu.edu.cn

contamination of drinking water and other natural water resources by Pb. Hence, new materials are required for not only selective detection of Pb^{2+} but also for its effective removal [5, 6]. Furthermore, intracellular or *in vivo* sensing of Pb^{2+} is required in biology and environmental toxicology [7].

To date, the majority of the Pb^{2+} detection and removal tasks have been performed separately. Traditional spectrometry, liquid chromatography, and electrochemical analysis enable accurate, sensitive, and reliable detection of Pb^{2+} [8–10]. However, these techniques usually require expensive equipment and tedious sample pretreatment; hence, they cannot be used for *in situ* and intracellular imaging. In recent years, several fluorescent probes for Pb^{2+} have been developed to clarify its cellular role *in vivo* as well as to monitor its temporal concentration in Pb^{2+}-contaminated sources [11, 12]. Nevertheless, in most cases, immobilization of these sensors at a high concentration has not been demonstrated, making it difficult to effectively remove Pb^{2+} at the same time. Thus, it is highly desirable to obtain a fluorescent probe possessing Pb^{2+} removal capabilities via a one-pot route, and achieve sensitive and selective detection of Pb^{2+} in biological and environmental samples.

Carbon dots (CDs) are newly emerging fluorescent nanomaterials that have attracted increasing interest due to their advantages such as facile preparation, biocompatibility, high photostability, water solubility, and tunable surface functional groups [13]. Diverse precursors, from small molecules (i.e., glucose, citrates) [14] to macromolecules [15] and renewable biological resources (i.e., grass, roses) [16, 17], have been used for the preparation of CDs. CDs usually inherit carboxyl, carbonyl, amino, amide, and hydroxyl groups from their precursors; thus, they have the ability to bind with metal ions, resulting in fluorescence quenching via the excited-state electron transfer mechanism [18]. At present, many studies have reported metal ion sensors using CDs as fluorescent probes [19]. For most of these sensors, as-prepared CDs are used as the probes and the selectivity for a certain metal ion is usually low [20–23]. High selectivity in some CD-based metal sensors has been achieved by tethering a selective ligand to the surface of the CDs [24, 25]; however, this process is burdensome and restricts large-scale production. Recently, as-prepared CDs with specific selective recognition abilities have emerged as a new hotspot in CD research [26, 27]. For instance, CDs derived from D-glucose and L-Asp exhibit significant capability for targeting C6 glioma cells without the need for any additional targeting molecules [26]. We speculate that the targeting function may originate from the formation of Arg-Gly-Asp (RGD) tripeptide-like moieties on the edge of the CDs during the synthesis. Interestingly, many studies have reported that natural flavonoids and their glycosides with some specific structural motifs can bind to Pb^{2+} with high selectivity [28–30]. Therefore, the synthesis of self-targeting CDs for Pb^{2+} detection using flavonoids as the starting material may lead to the development of a new type of metal ion sensors.

Herein, we synthesized a novel type of fluorescent CD (CD-Fla) via a one-pot hydrothermal route using flavonoid extracts of *Ginkgo biloba* leaves as the starting material. The fluorescence of as-prepared CD-Fla was selectively quenched by Pb^{2+} in water without any further modification. By contrast, CD-Sac, which was prepared from polysaccharide extracts of *G. biloba* leaves did not show an obviously higher selectivity for Pb^{2+} compared to that for other traditional metal ions. This work demonstrated that CD-Fla could act as a highly selective fluorescent probe for Pb^{2+} detection in water and intracellular Pb^{2+} detection. Furthermore, CD-Fla could be readily doped on agarose hydrogel via H-binding and dipole-dipole interactions. This CD-Fla-doped hydrogel allowed for simultaneous visual fluorescence detection and removal of Pb^{2+} from water. A sample-volume-dependent sensitivity has been demonstrated for ultrasensitive Pb^{2+} detection. In addition, the fluorescence of CD-Fla within the gel could be fully recovered after Pb^{2+} desorption, indicating that the gel was reusable.

2 Experimental

2.1 Materials and reagents

Fresh *G. biloba* leaves were collected from trees located in Chongqing University, cleaned, and dried to a constant weight. Lead acetate, mercury perchloride, copper sulfate, zinc chloride, magnesium chloride,

cobalt chloride, sodium chloride, potassium chloride, silver nitride, ferric sulfate, ferrous sulfate, and ethanol were obtained from Aladdin Industrial Corporation (Shanghai, China). Quinine sulfate and tris(hydroxymethyl) aminomethane (Tris) were purchased from Sigma-Aldrich (Beijing, China). All other reagents were of analytical reagent grade. All aqueous solutions were prepared using ultrapure water (18.2 MΩ·cm, Milli-Q, Millipore).

2.2 Typical synthesis of CDs

Flavonoid extraction from *G. biloba* leaves was performed according to a previously reported method with some modifications [31]. Specifically, the dried *G. biloba* leaves were first powdered, and 10.0 g of powder was added to 125 mL 75% (v/v) ethanol. After leaching for 2 h at 70 ℃, the mixture was filtered. The filter residues were collected for further use. The filtrate was concentrated by vacuum distillation; the concentrate was the flavonoid extract of *G. biloba* leaves. The extract was then mixed in 15 mL water, transferred to a high-temperature reaction kettle, and allowed to react hydrothermally for 5 h at 200 ℃. After cooling to room temperature, the reaction product was centrifuged at 8,000 rpm for 20 min to remove the precipitates. The supernatants were collected and dialyzed (3,000 D tubing) for 24 h to obtain final CD-Fla. The yield of CD-Fla from flavonoid extracts was calculated to be ca. 20% based on the weight of the lyophilized flavonoid extracts and CD-Fla.

The filter residues were washed with anhydrous ethanol (250 mL) and 75% (v/v) ethanol (350 mL) and then mixed in 150 mL water and heated to reflux for 2 h. Then, the mixture was filtered and the filtrate was concentrated by vacuum distillation to obtain polysaccharide extracts of *G. biloba* leaves [32]. The polysaccharide extracts were treated in the same manner as the flavonoid extracts to obtain CD-Sac. The yield of CD-Sac from the polysaccharide extracts was calculated to be ca. 30% based on the weight of the lyophilized polysaccharide extracts and CD-Sac.

2.3 Characterization

Fluorescence measurements were performed using a Shimadzu FL-7000 spectrofluorometer with a slit width of 5 nm for excitation and emission. Ultraviolet–visible spectroscopy (UV–vis) measurements were recorded on a Shimadzu UV-2600 UV-Vis spectrophotometer. Fourier transform infrared spectroscopy (FTIR) measurements were performed using a BRUKER Vertex 70 FTIR spectrometer with KBr pellets. Transmission electron microscopy (TEM) experiments were performed using a Philips Tacnai G2 20 S-TWIN microscope operating at 200 kV. For visualization by TEM, samples were prepared by dropping a solution of production on a copper grid. The fluorescence images were collected using a plate reader (Eppendorf AF2200; 485-nm excitation).

2.4 Preparation of CD-Fla doped agarose hydrogel (CD-AHG)

This preparation involved boiling of agarose gel with CD-Fla solution. Typically, 0.25 g of agarose gel was added to a 10 mL CD solution (10 mg·mL^{-1}), and the pH value was adjusted to 11 using 1 M NaOH. The mixture was then boiled for 5 min to complete solubilization of agarose. It was cooled to room temperature and cut into slices as required. The slices had an average diameter of 0.8 cm, thickness of 2 mm, hydrated weight of 93.6 mg, and dry weight of 3.2 mg. Each CD-AHG slice contained on average 0.91 mg CD-Fla. The slices were then soaked in water before use.

3 Results and discussion

Typically, CD-Fla was prepared from the flavonoid extracts of *G. biloba* leaves via a hydrothermal method (see the Experimental section for details). This extract contained three flavonoids, kaempferol, quercetin, and isohamnetin, and their respective glycosides (Scheme 1) [31]. Owing to the existence of saccharide moieties, as-prepared CD-Fla was hydrophilic and readily dispersible in water. For comparison, CD-Sac, which was prepared from the polysaccharide extracts of *G. biloba* leaves, was prepared using the same method. TEM observations were performed for the characterization of the structure and morphology of all the CDs. Figure 1(a) shows the typical TEM image of CD-Fla, revealing an average diameter of 4.18 ±

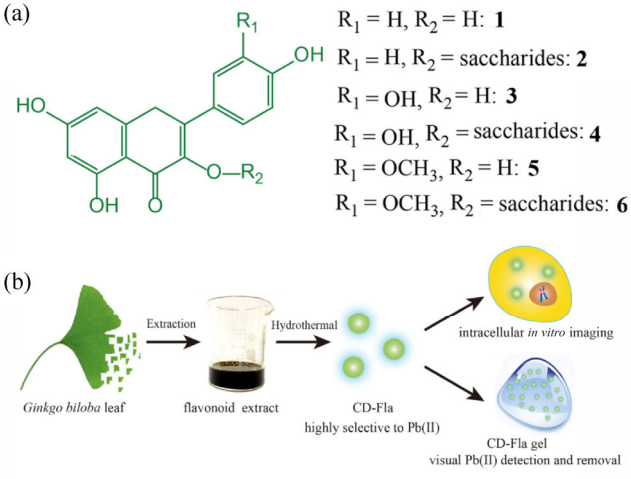

Scheme 1 (a) Main flavonoids and flavonoid glycosides in the flavonoid extracts of *Ginkgo biloba* leaves. Components: **1**, kaempferol; **2**, kaempferol glycosides; **3**, quercetin; **4**, quercetin glycosides; **5**, isohamnetin; and **6**, isohamnetin glycosides. (b) Schematic representation of the synthesis of CD-Fla and its applications.

1.14 nm (Fig. 1(b)). The high-resolution TEM image (Fig. 1(a), inset) indicates the crystallinity of CD-Fla with a lattice parameter of ca. 0.22 nm, which is in agreement with the basal spacing of graphite. This result confirmed that as-prepared CD-Fla has a crystalline graphite-like structure.

FTIR spectra were used to identify the chemical composition of CD-Fla. The FTIR spectra of CD-Fla and CD-Sac were obviously different. The vibration bands at 3,300 and 1,032 cm^{-1} representing the respective hydroxyl and C–O–C groups and depended on the starting material. As shown in Fig. 1(c), the relative intensity of the two vibration bands was weaker in the spectrum of CD-Fla than in that of CD-Sac. Most obviously, there was a strong vibration band at 1,742 cm^{-1} in the spectrum of CD-Fla, but it was not observed in that of CD-Sac. The vibration band at 1,742 cm^{-1} represented carbonyl groups (C=O), indicating that flavonoid-related moieties are incorporated into the structure of CD-Fla. Furthermore, the unique vibration bands between 400 and 800 cm^{-1} in the spectrum of CD-Fla confirmed the existence of flavonoid-related moieties (Fig. 1(c)). Signals for

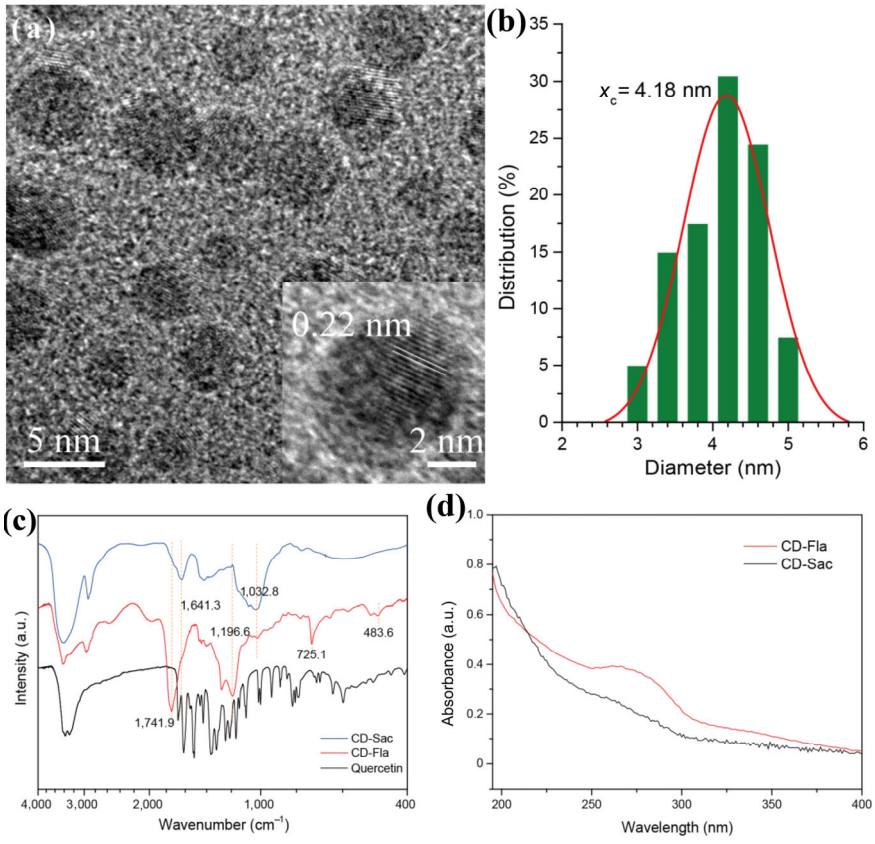

Figure 1 (a) TEM image of CD-Fla (inset: high-resolution TEM image of CD-Fla); (b) Diameter distribution of CD-Fla measured by TEM; (c) FTIR spectra of CD-Fla, CD-Sac, and quercetin; (d) UV–vis spectra of CD-Fla and CD-Sac.

flavonoid moieties were not observed in the spectrum of CD-Sac Wide absorption bands around 270–300 nm were observed in the UV–vis absorption spectrum (Fig. 1(d)) of CD-Fla only and originated from the π–π* and n–π* transitions of flavonoid-related moieties such as polyaromatic chromophores and carbonyl groups, respectively. Both CD-Fla and CD-Sac exhibited blue fluorescence under UV light excitation; their fluorescence spectra are shown in Fig. S1 in the Electronic Supplementary Material (ESM). CD-Fla and CD-Sac also exhibited excitation-dependent emission properties similar to other reported ones [14]. The maximum excitation wavelength and fluorescence quantum yield for CD-Fla and CD-Sac was 350 and 360 nm and 16.1% and 9.3%, respectively, according to our previously reported method [14]. The *in vitro* (3-(4,5-dimethylthiazol-2-yl)-2,5-diphenyltetrazolium bromide) (MTT) assay suggested that even at high concentrations, CD-Fla was noncytotoxic to HeLa cells (Fig. S2 in the ESM).

The fluorescence response of CD-Fla to Pb^{2+} was then investigated. Fluorescence measurements were performed in a 1.0 μg·mL^{-1} CD-Fla aqueous solution maintained at a pH of 7.5 using 10 mM Tris-HCl solution. As shown in Fig. 2(a), the fluorescence intensity of CD-Fla was quenched in proportion with the Pb^{2+} concentration from 0.2 nM to 50.0 mM. The suitability of such a Pb^{2+} concentration-dependent fluorescence variation system for the detection of Pb^{2+} was then evaluated. Fig. 2(b) shows the relationship between the varying fluorescence intensity of CD-Fla at 440 nm ($\Delta I_{440nm} = I_0 - I$) and Pb^{2+} concentration. Favorable linear correlations ($R^2 > 0.96$) existed between ΔI_{440nm} and Pb^{2+} concentration over the range of 0.1–20.0 nM (Fig. 2(b) inset). Based on 3σ/slope, the limit of Pb^{2+} detection was estimated to be about 55 pM. As shown in Table S1 in the ESM, the Pb^{2+} detection sensitivity of this method was much higher than those of some recently reported luminescent chemo- [33, 34] and nanosensors [35–39] and comparable to that of signal-amplified electrochemical aptosensors [40].

The selectivity of CD-Fla for Pb^{2+} compared to that for some environmentally relevant metal ions (including Na^+, K^+, Co^{2+}, Hg^{2+}, Ag^+, Cu^{2+}, Fe^{2+}, Fe^{3+}, Zn^{2+}, and Mg^{2+}) was investigated. The fluorescence response

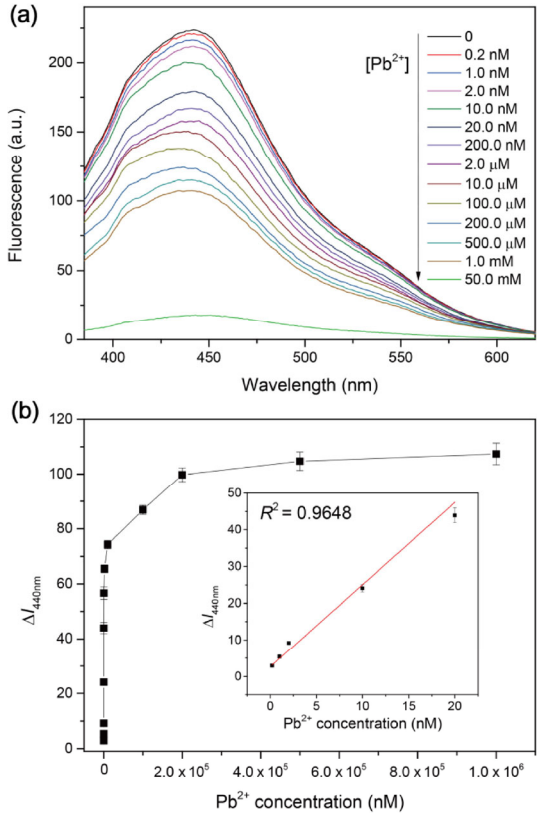

Figure 2 (a) Fluorescence spectra of CD-Fla in the presence of different concentrations of Pb^{2+} from 0.2 nM to 50 mM. Excitation = 360 nm. (b) Plot for fluorescence variation (ΔI_{440nm}) versus Pb^{2+} concentration; the inset shows the linear relationship between ΔI_{440nm} and Pb^{2+} concentration within the concentration range of 0.2 to 20 nM.

of CD-Fla to Pb^{2+} presented better selectivity that for other metal ions. As indicated in Fig. 3, unlike the significant fluorescence response observed in the presence of Pb^{2+}, no significant variations in fluorescence intensity were observed upon the addition of the same concentration of the other metal ions. Therefore, CD-Fla could serve as a promising fluorescent probe for Pb^{2+} detection because of its low selectivity to other metal ions.

Furthermore, to investigate possible factors determining the selectivity of CD-Fla for Pb^{2+}, the fluorescence response of CD-Sac to different metal ions was measured as control experiments. Consequently, the fluorescence of CD-Sac was affected slightly by the addition of 10 nM of other metal ions (Fig. 3), indicating that CD-Sac does not target Pb^{2+} alone. As previously reported, Pb^{2+} could bind to flavonoid diglycosides with different dissociation constants; this

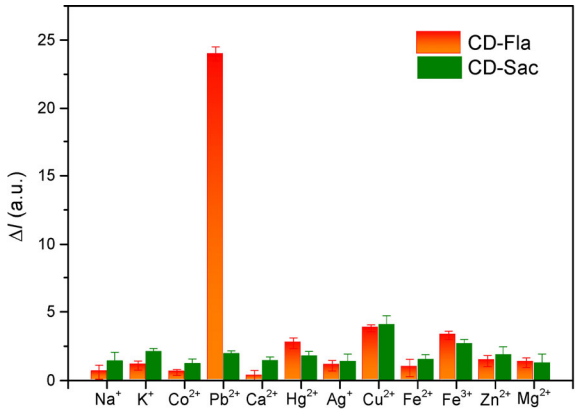

Figure 3 Effect of 10 nM of different metal ions on the fluorescence quenching of CD-Fla and CD-Sac. The fluorescence variation ($\Delta I = I_0 - I$) was monitored at 440 and 421 nm for CD-Fla and CD-Sac, respectively.

property has been used to target specific structural motifs of flavonoid glycosides [29]. Interestingly, a flavonoid motif-based ligand has been designed to selectively bind Pb^{2+} [30]. In our present work, we speculate about the selective binding ability of CD-Fla because of the formation of Pb^{2+}-specific flavonoid-based motifs on its edges during the preparation of CDs from flavonoid extracts (containing flavonoids and flavonoid glycosides, as shown in Scheme 1). Spectroscopic characterizations conducted above have confirmed that CD-Fla contains flavonoid-relevant motifs (Figs. 1(c) and 1(d)). Some recent studies have also proved the rationality of retention and formation of some functional groups on CD edges from specific starting materials via pyrolysis. For instance, Zheng et al. reported a brain cancer glioma targeting CD due to the formation of RGD, a triple peptide-like motif on its edge from the precursors D-glucose and L-aspartic acid [26]. Furthermore, a recent study has reported a bacteria-derived CD capable of differentiating between live and dead microbials [27]. Therefore, direct preparation of functional CDs from specific starting materials is a major CD research trend, and our present study matches this well. A more detailed study of Pb^{2+} targeting mechanism of CD-Fla is ongoing.

The feasibility of using CD-Fla for cellular staining and intracellular Pb^{2+} tracing was also investigated. HeLa cells were incubated with CD-Fla for 2 h and washed with PBS buffer to remove free CD-Fla in the solution and prevent any nonspecific adsorption on the cell surface. The fluorescence microscopy images showed that the cytoplasm of the HeLa cell was clearly stained with the blue fluorescence of CD-Fla (Fig. 4(a)). The result indicated that CD-Fla can easily penetrate into cells and can be used as a benign intracellular Pb^{2+} probe. To prove this, the cells incubated with CD-Fla were treated with Pb^{2+} for another 2 h. As shown in Figs. 4(b) and 4(c), the fluorescence intensity obviously weakened with an increase in Pb^{2+} concentration, demonstrating that CD-Fla can be used to track changes in intracellular Pb^{2+} levels in mammalian cells.

Considering the ultrahigh sensitivity and selectivity of CD-Fla for Pb^{2+}, it was doped on agarose hydrogel (AHG) for fluorescence visible detection and removal of Pb^{2+} from water. CD-AHG was cut into slices as required. No observable CD-Fla leakage was found by soaking the CD-AHG slices in water for one week because of the multivalent H-bonding between the CD-Fla and agarose matrices. The as-prepared CD-AHG slices showed high blue fluorescence under a UV lamp (365 nm). The blue fluorescence of CD-AHG

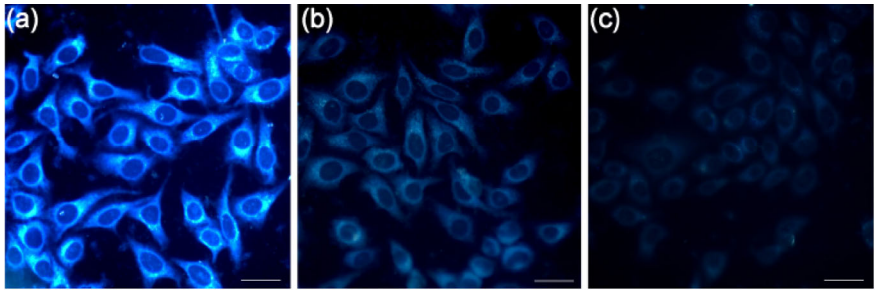

Figure 4 (a) Fluorescence images of HeLa cells incubated with CD-Fla; images of CD-Fla incubated HeLa cells after incubation with (b) 1 μM and (c) 10 μM Pb^{2+} for 2 h. Scale bar = 25 μm.

was quenched by soaking it in Pb^{2+} solution. Similar to the CD-Fla-in-solution system, the fluorescence of the CD-Fla doped on CD-AHG was also quenched by Pb^{2+}. To determine the optimal detection time, we investigated the kinetics of fluorescence change. As shown in Fig. 5(a), the fluorescence of CD-AHG was quenched rapidly and obviously within 30 min in 100 nM Pb^{2+} solution. The fluorescence quenching tended to become steady over the course of 50 min; hence, this time was chosen as the optimal detection time for subsequent experiments.

To evaluate the sensitivity of the hydrogel-based sensor, the CD-AHG slices were soaked in varying concentrations of Pb^{2+} for 50 min. The blue fluorescence quenching of CD-AHG was investigated by soaking one CD-AHG slice in 1 mL water solution with varying Pb^{2+} concentrations, from 5 to 100 nM. As shown in Fig. 5(b), the blue fluorescence was gradually quenched with increasing Pb^{2+} concentration. About 10 nM Pb^{2+} led to visual detection, thus allowing very sensitive and facile monitoring of Pb^{2+} in water systems. Such a gel system also allowed quantitative analysis of Pb^{2+} by simply collecting the fluorescence intensity of CD-AHG slices soaked in Pb^{2+} solution with a CCD camera (Fig. S3 in the ESM). We investigated the Pb^{2+} adsorption capability of CD-Fla alone using ultrafiltration due to the well-known complexation ability between the flavonoid moieties in CD-Fla and Pb^{2+} [28–30]. The maximum adsorption amount was determined to be 0.35 mg Pb^{2+} per milligram of CD-Fla. Thus, we expected that CD-AHG could also adsorb Pb^{2+}. Therefore, the fluorescence response sensitivity of CD-AHG could be increased by simply increasing the sample volume. To test this hypothesis, the CD-AHG slices were soaked in 50 mL of 0.5 nM Pb^{2+} solution (previously 1 mL). As shown in Fig. S4 in the ESM, even 0.5 nM Pb^{2+} induced easily visible fluorescence quenching. This sensitivity is among the highest of all reported Pb^{2+} sensors with no analytical instruments or signal amplification methods used for detection [18, 19]. This gel-based sensor is expected to be practically useful because the maximum contamination level of Pb^{2+} defined by the U.S. Environmental Protection Agency (EPA) is no more than 72 nM. The selectivity of CD-AHG was also tested by incubating the CD-AHG slices with various metal ions, and only Pb^{2+} produced significant fluorescence quenching (Fig. S5 in the ESM), suggesting that high selectivity of CD-Fla for Pb^{2+} is maintained within the hydrogel matrix.

The unique volume-dependent sensitivity of CD-AHG confirms that AHG can actively adsorb and remove Pb^{2+} from water. To study the Pb^{2+} adsorption and removal ability, 10 slices of CD-AHG and agarose hydrogel were separately soaked in 1 μM (10 mL Tris-HCl buffer) Pb^{2+} solutions. The supernatant solutions after hydrogel treatment were acidified and analyzed by ICP-MS as an independent verification. As shown in Fig. 6, the lead concentration in the Pb^{2+} solution with CD-AHG slices was 29.8 nM after adsorption of CD-AHG, whereas that in the Pb^{2+} solution with agarose hydrogel slices was as high as 860.6 nM after the adsorption of agarose hydrogel. The results suggested that agarose hydrogel matrices have weak Pb^{2+} adsorption ability, whereas CD-AHG is a cost-effective and safe Pb^{2+} removal candidate. According to the data from Fig. 6, the maximum

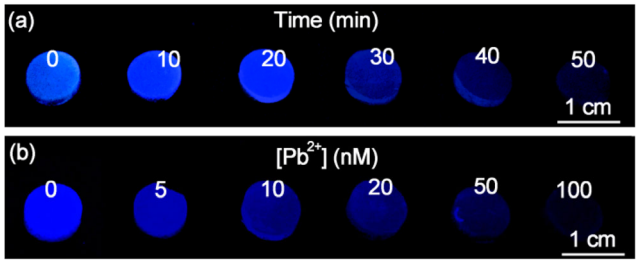

Figure 5 (a) CD-AHG gel fluorescence change in 100 nM Pb^{2+} solution as a function of time; (b) fluorescence of CD-AHG with different Pb^{2+} concentrations.

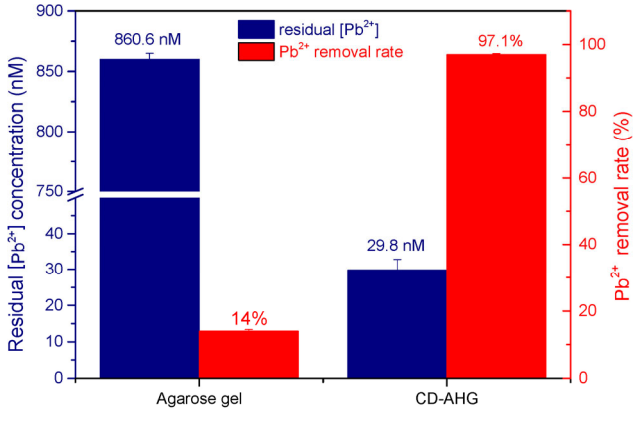

Figure 6 Residual lead concentrations after agarose gel and CD-AHG treatment and the corresponding Pb^{2+} removal rate (%); 10 gel slices in 1 μM (10 mL Tris-HCl buffer) Pb^{2+} solution.

Pb^{2+} adsorption of CD-AHG was calculated to be 0.20 mg/slice.

To evaluate the practical applicability of CD-AHG, environmental water samples from the Jialing River (Chongqing, China) were tested. Since lead was not detected in these water samples by ICP-MS, Pb^{2+} was deliberately added to simulate contaminated water. Each slice of CD-AHG was soaked in 10 mL of the water. After CD-AHG treatment, the supernatants were collected and analyzed using ICP-MS for lead. The Pb^{2+} concentration showed an obvious decrease from 100 to 2.39 nM, indicating that CD-AHG is capable of Pb^{2+} removal in natural water. The detection sensitivity of this gel-based sensor for Pb^{2+} was also investigated. The obtained limit of detection was 12.89 nM (1 mL sample volume). This sensitivity was slightly lower than that obtained in the Tris-HCl buffer solution. This may be attributed to the coexistence of anions (such as phosphate and sulfate anions), which can form complexes with Pb^{2+}. These results clearly demonstrated that CD-AHG is capable of detecting and removing Pb^{2+} from environmental water samples.

The immobilized CD-Fla within the agarose hydrogel matrix regenerates. To evaluate this, CD-AHG adsorbed with Pb^{2+} was soaked with 0.5 M HCl for 10 min and then soaked in a buffer solution for 30 min; this process was repeated 5 times. Subsequently, the adsorbed Pb^{2+} was removed from CD-AHG, implying that CD-AHG was regenerated. This was confirmed by the change in fluorescence behavior: CD-AHG adsorbed with Pb^{2+} was non-fluorescent (Fig. S6(a) in the ESM), while the recovered CD-AHG exhibited fluorescence (Fig. S6(b) in the ESM) that could still be sensitively quenched by soaking with a Pb^{2+} solution (Fig. S6(c) in the ESM).

4 Conclusions

In summary, CD-Fla was synthesized by a facile one-pot hydrothermal route using flavonoid extracts of *G. biloba* leaves as the starting material. CD-Fla was biologically benign and highly fluorescent and exhibited a self-targeting function for Pb^{2+}, and could be used as an ultrasensitive fluorescent probe for Pb^{2+} in water as well as intracellular Pb^{2+}. The capability of CD-Fla could be further improved by doping it on agarose hydrogel. The gel could achieve visible detection and removal of Pb^{2+} both in buffer samples and environmental water samples. The detection sensitivity of this gel sensor could be improved by using a larger sample volume. This work demonstrated that CDs could be used as a platform for synthesizing integrated nanomaterials capable of ultrasensitive, highly selective detection of Pb^{2+} in all cases and removal of Pb^{2+} from environmental water samples. It provides a new path for direct preparation of functional CDs, especially for potential development of CD-based sensors from other metal-specific chelators.

Acknowledgements

Financial support was provided by the National Natural Science Foundation of China (No. 21675016), Chongqing Basic and Frontier Research Program (No. cstc2016jcyjA0328), and the 100 Young Plan by Chongqing University (No. 0236011104410).

Electronic Supplementary Material: Supplementary material (fluorescent spectra of CDs, MTT assay, and some CD-AHG gel based data) is available in the online version of this article at https://doi.org/10.1007/s12274-017-1931-6.

References

[1] Mikac, N.; Branica, M.; Wang, Y.; Harrison, R. M. Organolead compounds in mussels (*Mytilus galloprovincialis*) from the eastern Adriatic coast. *Environ. Sci. Technol.* **1996**, *30*, 499–508.

[2] Turpeinen, R.; Salminen, J.; Kairesalo, T. Mobility and bioavailability of lead in contaminated boreal forest soil. *Environ. Sci. Technol.* **2000**, *34*, 5152–5156.

[3] Bellinger, D. C.; Needleman, H. L. Intellectual impairment and blood lead levels. *N. Engl. J. Med.* **2003**, *349*, 500–502.

[4] Sun, J. T.; Yu, G. X.; Zhang, Y. C.; Liu, X.; Du, C.; Wang, L.; Li, Z.; Wang, C. H. Heavy metal level in human semen with different fertility: A meta-analysis. *Biol. Trace Elem. Res.* **2017**, *176*, 27–36.

[5] Babel, S.; Kurniawan, T. A. Low-cost adsorbents for heavy metals uptake from contaminated water: A review. *J. Hazard. Mater.* **2003**, *97*, 219–243.

[6] Kim, H. N.; Ren, W. X.; Kim, J. S.; Yoon, J. Fluorescent and colorimetric sensors for detection of lead, cadmium,

and mercury ions. *Chem. Soc. Rev.* **2012**, *41*, 3210–3244.

[7] Grąz, M.; Pawlikowska-Pawlęga, B.; Jarosz-Wilkołazka, A. Growth inhibition and intracellular distribution of Pb ions by the white-rot fungus *Abortiporus biennis*. *Int. Biodeterior. Biodegrad.* **2011**, *65*, 124–129.

[8] Ghaedi, M.; Shokrollahi, A.; Niknam, K.; Niknam, E.; Najibi, A.; Soylak, M. Cloud point extraction and flame atomic absorption spectrometric determination of cadmium(II), lead(II), palladium(II) and silver(I) in environmental samples. *J. Hazard. Mater.* **2009**, *168*, 1022–1027.

[9] Shum, S. C. K.; Pang, H. M.; Houk, R. S. Speciation of mercury and lead compounds by microbore column liquid chromatography-inductively coupled plasma mass spectrometry with direct injection nebulization. *Anal. Chem.* **1992**, *64*, 2444–2450.

[10] Xiao, Y.; Rowe, A. A.; Plaxco, K. W. Electrochemical detection of parts-per-billion lead via an electrode-bound DNAzyme assembly. *J. Am. Chem. Soc.* **2007**, *129*, 262–263.

[11] Gupta, A.; Verma, N. C.; Khan, S.; Tiwari, S.; Chaudhary, A.; Nandi, C. K. Paper strip based and live cell ultrasensitive lead sensor using carbon dots synthesized from biological media. *Sens. Actuator B-Chem.* **2016**, *232*, 107–114.

[12] Kuo, S. Y.; Li, H. H.; Wu, P. J.; Chen, C. P.; Huang, Y. C.; Chan, Y. H. Dual colorimetric and fluorescent sensor based on semiconducting polymer dots for ratiometric detection of lead ions in living cells. *Anal. Chem.* **2015**, *87*, 4765–4771.

[13] Zhu, S. J.; Song, Y. B.; Zhao, X. H.; Shao, J. R.; Zhang, J. H.; Yang, B. The photoluminescence mechanism in carbon dots (graphene quantum dots, carbon nanodots, and polymer dots): Current state and future perspective. *Nano Res.* **2015**, *8*, 355–381.

[14] Wei, W. L.; Xu, C.; Wu, L.; Wang, J. S.; Ren, J. S.; Qu, X. G. Non-enzymatic-browning-reaction: A versatile route for production of nitrogen-doped carbon dots with tunable multicolor luminescent display. *Sci. Rep.* **2014**, *4*, 3564.

[15] Wee, S. S.; Ng, Y. H.; Ng, S. M. Synthesis of fluorescent carbon dots via simple acid hydrolysis of bovine serum albumin and its potential as sensitive sensing probe for lead (II) ions. *Talanta* **2013**, *116*, 71–76.

[16] Liu, S.; Tian, J. Q.; Wang, L.; Zhang, Y. W.; Qin, X. Y.; Luo, Y. L.; Asiri, A. M.; Al-Youbi, A. O.; Sun, X. P. Hydrothermal treatment of grass: A low-cost, green route to nitrogen-doped, carbon-rich, photoluminescent polymer nanodots as an effective fluorescent sensing platform for label-free detection of Cu(II) ions. *Adv. Mater.* **2012**, *24*, 2037–2041.

[17] Feng, Y. J.; Zhong, D.; Miao, H.; Yang, X. M. Carbon dots derived from rose flowers for tetracycline sensing. *Talanta* **2015**, *140*, 128–133.

[18] Zhang, J. J.; Cheng, F. F.; Li, J. J.; Zhu, J. J.; Lu, Y. Fluorescent nanoprobes for sensing and imaging of metal ions: Recent advances and future perspectives. *Nano Today* **2016**, *11*, 309–329.

[19] Gao, X. H.; Du, C.; Zhuang, Z. H.; Chen, W. Carbon quantum dot-based nanoprobes for metal ion detection. *J. Mater. Chem. C* **2016**, *4*, 6927–6945.

[20] Gogoi, N.; Barooah, M.; Majumdar, G.; Chowdhury, D. Carbon dots rooted agarose hydrogel hybrid platform for optical detection and separation of heavy metal ions. *ACS Appl. Mater. Interfaces* **2015**, *7*, 3058–3067.

[21] Wen, X. P.; Shi, L. H.; Wen, G. M.; Li, Y. Y.; Dong, C.; Yang, J.; Shuang, S. M. Green synthesis of carbon nanodots from cotton for multicolor imaging, patterning, and sensing. *Sens. Actuator B-Chem.* **2015**, *221*, 769–776.

[22] Tan, X. W.; Romainor, A. N. B.; Chin, S. F.; Ng, S. M. Carbon dots production via pyrolysis of sago waste as potential probe for metal ions sensing. *J. Anal. Appl. Pyrolysis* **2014**, *105*, 157–165.

[23] Liu, Y. Y.; Kim, D. Y. Ultraviolet and blue emitting graphene quantum dots synthesized from carbon nano-onions and their comparison for metal ion sensing. *Chem. Commun.* **2015**, *51*, 4176–4179.

[24] Yuan, C.; Liu, B. H.; Liu, F.; Han, M. Y.; Zhang, Z. P. Fluorescence "turn on" detection of mercuric ion based on bis(dithiocarbamato)copper(II) complex functionalized carbon nanodots. *Anal. Chem.* **2014**, *86*, 1123–1130.

[25] Zhu, A. W.; Qu, Q.; Shao, X. L.; Kong, B.; Tian, Y. Carbon-dot-based dual-emission nanohybrid produces a ratiometric fluorescent sensor for *in vivo* imaging of cellular copper ions. *Angew. Chem., Int. Ed.* **2012**, *51*, 7185–7189.

[26] Zheng, M.; Ruan, S. B.; Liu, S.; Sun, T. T.; Qu, D.; Zhao, H. F.; Xie, Z. G.; Gao, H. L.; Jing, X. B.; Sun, Z. C. Self-targeting fluorescent carbon dots for diagnosis of brain cancer cells. *ACS Nano* **2015**, *9*, 11455–11461.

[27] Hua, X. W.; Bao, Y. W.; Wang, H. Y.; Chen, Z.; Wu, F. G. Bacteria-derived fluorescent carbon dots for microbial live/dead differentiation. *Nanoscale* **2017**, *9*, 2150–2161.

[28] Ravichandran, R.; Rajendran, M.; Devapiriam, D. Structural characterization and physicochemical properties of quercetin–Pb complex. *J. Coord. Chem.* **2014**, *67*, 1449–1462.

[29] Ilboudo, O.; Tapsoba, I.; Bonzi-Coulibaly, Y. L.; Gerbaux, P. Targeting structural motifs of flavonoid diglycosides using collision-induced dissociation experiments on flavonoid/Pb^{2+} complexes. *Eur. J. Mass Spectrom.* **2012**, *18*, 465–473.

[30] Lanoe, P. H.; Fillaut, J. L.; Toupet, L.; Williams, J. A. G.; Le Bozec, H.; Guerchais, V. Cyclometallated platinum(II) complexes incorporating ethynyl-flavone ligands: Switching between triplet and singlet emission induced by selective

binding of Pb^{2+} ions. *Chem. Commun.* **2008**, 4333–4335.

[31] van Beek, T. A.; Montoro, P. Chemical analysis and quality control of *Ginkgo biloba* leaves, extracts, and phytopharmaceuticals. *J. Chromatogr. A* **2009**, *1216*, 2002–2032.

[32] Kraus, J. Water-soluble polysaccharides from *Ginkgo biloba* leaves. *Phytochemistry* **1991**, *30*, 3017–3020.

[33] Xu, B. H.; Tang, X. L.; Zhou, J. A.; Chen, W. M.; Liu, H. L.; Ju, Z. H.; Liu, W. S. A "turn-on" lanthanide complex chemosensor for recognition of lead(II) based on the formation of nanoparticles. *Dalton Trans.* **2016**, *45*, 18859–18866.

[34] Yu, Z.; Zhou, W.; Han, J.; Li, Y. C.; Fan, L. Z.; Li, X. H. Na^{+}-induced conformational change of Pb(II)-stabilized g-quadruplex and its influence on Pb^{2+} detection. *Anal. Chem.* **2016**, *88*, 9375–9380.

[35] Zhang, Y. F.; Maimaiti, H.; Zhang, B. Preparation of cellulose-based fluorescent carbon nanoparticles and their application in trace detection of Pb(II). *RSC Adv.* **2017**, *7*, 2842–2850.

[36] Chen, J. L.; Zhu, Y. X.; Zhang, Y. Glutathione-capped Mn-doped ZnS quantum dots as a room-temperature phosphorescence sensor for the detection of Pb^{2+} ions. *Spectroc. Acta Pt. A-Mol. Biomol. Spectr.* **2016**, *164*, 98–102.

[37] Liu, Y. L.; Zhou, Q. X.; Li, J.; Lei, M.; Yan, X. Y. Selective and sensitive chemosensor for lead ions using fluorescent carbon dots prepared from chocolate by one-step hydrothermal method. *Sens. Actuator B-Chem.* **2016**, *237*, 597–604.

[38] Qian, Z. S.; Shan, X. Y.; Chai, L. J.; Chen, J. R.; Peng, H. A fluorescent nanosensor based on graphene quantum dots-aptamer probe and graphene oxide platform for detection of lead(II) ion. *Biosens. Bioelectron.* **2015**, *68*, 225–231.

[39] Xu, S.; Xu, S. H.; Zhu, Y. S.; Xu, W.; Zhou, P. W.; Zhou, C. Y.; Dong, B.; Song, H. W. A novel upconversion, fluorescence resonance energy transfer biosensor (FRET) for sensitive detection of lead ions in human serum. *Nanoscale* **2014**, *6*, 12573–12579.

[40] Zhang, C.; Lai, C.; Zeng, G. M.; Huang, D. L.; Tang, L.; Yang, C. P.; Zhou, Y. Y.; Qin, L.; Cheng, M. Nanoporous Au-based chronocoulometric aptasensor for amplified detection of Pb^{2+} using DNAzyme modified with Au nanoparticles. *Biosens. Bioelectron.* **2016**, *81*, 61–67.